

NUCLEAR SPECTROSCOPY OF VERY PROTON RICH NUCLEI THROUGH H.I. INDUCED REACTIONS;  
 THE 14s HIGH SPIN ISOMER IN  $^{95}\text{Pd}$

E. Nolte, G. Korschinek, H. Hick, G. Colombo, P. Komninos, S.Z. Gui, W. Schollmeier,  
 P. Kubik, R. Geier, U. Heim and H. Morinaga  
 Fachbereich Physik, Technische Universität München, Garching, Fed. Rep. Germany

Abstract

$^{40}\text{Ca}$ ,  $^{58}\text{Ni}$  and  $^{60}\text{Ni}$  beams from the Munich tandem and the Munich heavy ion postaccelerator have been used to produce very proton rich nuclei in the N=50 and N=82 regions. The residual nuclei have been studied with the help of  $\gamma$  and particle spectroscopy. The level schemes of  $^{95}\text{Rh}$ ,  $^{146}\text{Dy}$  and  $^{150}\text{Er}$  and the  $\beta$ -decay schemes  $^{95}\text{Pd}^m \rightarrow ^{95}\text{Rh}$ ,  $^{144}\text{Tb} \rightarrow ^{144}\text{Gd}$ ,  $^{146}\text{Ho} \rightarrow ^{146}\text{Dy}$ ,  $^{146}\text{Tb} \rightarrow ^{146}\text{Gd}$ ,  $^{148}\text{Er} \rightarrow ^{148}\text{Ho} \rightarrow ^{148}\text{Dy}$  and  $^{150}\text{Tm} \rightarrow ^{150}\text{Er} \rightarrow ^{150}\text{Ho} \rightarrow ^{150}\text{Dy}$  have been investigated.  $\beta$  delayed proton emission from a  $J^\pi \approx 21^+$  isomeric state in  $^{95}\text{Pd}$  has been observed.

$^{40}\text{Ca} \rightarrow ^{58}\text{Ni}$	133...173 MeV
$^{58}\text{Ni} \rightarrow ^{90}\text{Zr}, ^{92}\text{Mo}, ^{94}\text{Mo}$	230...250 MeV
$^{60}\text{Ni} \rightarrow ^{92}\text{Mo}$	240...259 MeV

In order to obtain the higher energies of the Ca beam and for the Ni beams the heavy ion postaccelerator<sup>1,2)</sup> was used. This postaccelerator is a linear RF accelerator of the Interdigital H-type structure. Its total accelerating voltage is about 5 MV which results in an energy increase of the beam of about 70%. The RF power for this voltage is about 33 kW. For a current of 100 nA of negative ions injected into the tandem the target current is 1 part.nA.

1. Introduction

By shooting  $^{40}\text{Ca}$  or  $^{58}\text{Ni}$  ion beams on lightest isotopes of medium heavy elements, one can produce compound nuclei far off the stability line. At beam energies just above the Coulomb barrier the excitation energies of the compound nuclei are so low that only a few particles - mainly protons - are evaporated and that only a few evaporation channels are open. In the case of  $^{58}\text{Ni} \rightarrow ^{94}\text{Mo}$  for instance, at a beam energy just above the Coulomb barrier the two proton evaporation is the strongest channel, essentially contaminated only by the 3p channel. Very proton rich nuclei still far off stability line can be produced in this way with reaction cross section which are by far larger than those for (H.I.,xn) reactions producing the same residual nuclei.

Since several years in the Munich tandem laboratory heavier heavy ion beams from  $^{32}\text{S}$  to  $^{70}\text{Ge}$  have been accelerated up to energies of 4.3 MeV/n by the combination MP tandem-heavy ion postaccelerator. This facility gives us the opportunity to study very proton rich nuclei with the help of in-beam  $\gamma$  ray spectroscopy, the investigation of the residual activities and the determination of nuclear masses. For several neutron deficient residual nuclei the  $Q_{EC} - B_p$  values are so high that  $\beta$  delayed proton emission can be expected. The study of this process gives additional spectroscopic information.

In the actual contribution we present results in the N=50 region and preliminary results in the N=82 region. In more detail we report the  $\beta$  delayed proton emission from a 14s high-spin isomer in  $^{95}\text{Pd}$ .

2. Experimental Set-Up and Procedure

$^{40}\text{Ca}$ ,  $^{58}\text{Ni}$  and  $^{60}\text{Ni}$  beams from the Munich MP tandem and from the postaccelerator were used to study the following projectile-target system:

The residual nuclei were studied with the following methods:

- $\gamma$  ray excitation functions
- prompt and delayed  $\gamma\gamma$  coincidences
- $\gamma$  Doppler shift life time measurements
- $\gamma$  ray and proton multi spectrum analysis' of the residual activities
- delayed coincidences between  $\beta$  delayed protons and  $\gamma$  rays
- pulsed beam technique
- bunched beam technique
- determination of nuclear masses with the help of the measurement of the  $K/\beta$  ratio

The  $\beta$  delayed protons were studied in the case  $^{135}\text{MeV } ^{40}\text{Ca} \rightarrow ^{58}\text{Ni}$  ( $360 \mu\text{g}/\text{cm}^2$ ). The residual nuclei recoiling from the target were slowed down by a  $7 \text{ mg}/\text{cm}^2$  Au foil and captured on a thin Ta foil mounted on a wheel. The wheel transported the activities within 1s in front of a particle detector and a coaxial Ge(Li) detector in  $180^\circ$  geometry. The particle detector was a Si surface barrier detector  $200 \mu\text{m}$  thick and with an active area of  $200 \text{ mm}^2$ . Proton and  $\gamma$  ray multi spectrum analysis' were performed. Delayed coincidences between  $\beta$  delayed protons and  $\gamma$  rays were taken.

For the investigation of isomeric life times in the 100 ms range a  $\gamma$  multi spectrum analysis was performed with a pulsed beam. The pulsed beam was obtained by pulsing the RF of the booster.

For the study of isomeric life times in the  $\mu\text{sec}$  range a bunched beam technique was used. In this case the ion beams were bunched with the help of the chopping and bunching system on the low energy side of the tandem. These beam bunches were re-bunched by the RF buncher on the high energy side of the tandem and injected into the postaccelerator. The distance between successive bunches was chosen to be  $13 \mu\text{s}$ .

### 3. Results

#### 3.1 N=50 Region

Very proton rich isotones with N=50 and neighbouring nuclei were studied with the system  $^{40}\text{Ca} \rightarrow ^{58}\text{Ni}$ . The compound nucleus is  $^{98}\text{Cd}_{50}$  which has only two protons less than the double-magic  $^{100}\text{Sn}$ . At a beam energy of 135 MeV the strongest channels are 4p ( $^{94}\text{Ru}$ ) and 3p ( $^{95}\text{Rh}$ ). The yields of all identified residual nuclei are drawn in Fig. 1. A part of the results on  $^{92}\text{Ru}$ ,  $^{94}\text{Ru}$  and  $^{95}\text{Rh}$  <sup>3)</sup> and preliminary results on  $^{95}\text{Pd}^m$  <sup>4)</sup> have been already published.

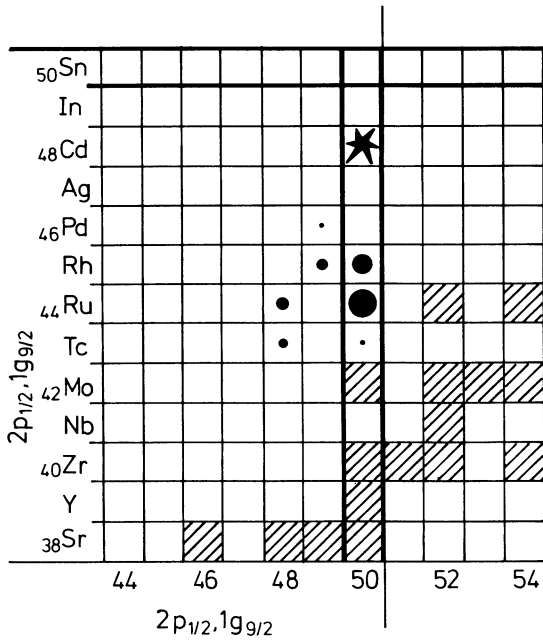


Fig. 1 Relevant part of the nuclear chart with the N=50 region. The compound nucleus of the system  $^{40}\text{Ca} \rightarrow ^{58}\text{Ni}$  is  $^{98}\text{Cd}$  (star). Circles indicate the yields of the residual nuclei at a beam energy of 135 MeV.

#### 3.1.1 The Level Scheme of $^{95}\text{Rh}$

The level scheme of  $^{95}\text{Rh}$  <sup>3)</sup> deduced with in-beam  $\gamma$  spectroscopic methods is shown in Fig. 2. Two cascades were identified: a positive parity band with the states  $(9/2^+)$ ,  $(13/2^+)$ ,  $(17/2^+)$ ,  $(21/2^+)$ ,  $(25/2^+)$  and higher lying levels and a negative parity band with the states  $(17/2^-)$ ,  $(21/2^-)$ ,  $(25/2^-)$  and higher lying levels. The  $(17/2^-)$  state decays to the  $(17/2^+)$  state. The half-life of the  $(17/2^-)$  state was measured to be  $15 \pm 5$  ns, the half-life of the  $(21/2^+)$  state was determined to be  $2.1 \pm 0.3$  ns. The corresponding  $B(E2; 21/2^+ \rightarrow 17/2^+)$  value is  $1.3 \pm 0.2$  w.u. The levels up to  $J = 25/2$  can be well described in the shell model with  $^{100}\text{Sn}$  as core and holes in the  $(\pi 2p_{1/2}, 1g_{9/2})$  subshell. The states  $9/2^+$  to  $25/2^+$  can be obtained from  $(g_{9/2})_{\nu}^{-5}$  configurations ( $\nu=1,3,5$ ) and the states  $17/2^-$  to  $25/2^-$  from  $(p_{1/2})_{\nu}^{-1}$ .  $(g_{9/2})_{\nu}^{-4}$  configurations ( $\nu=2,4$ ).

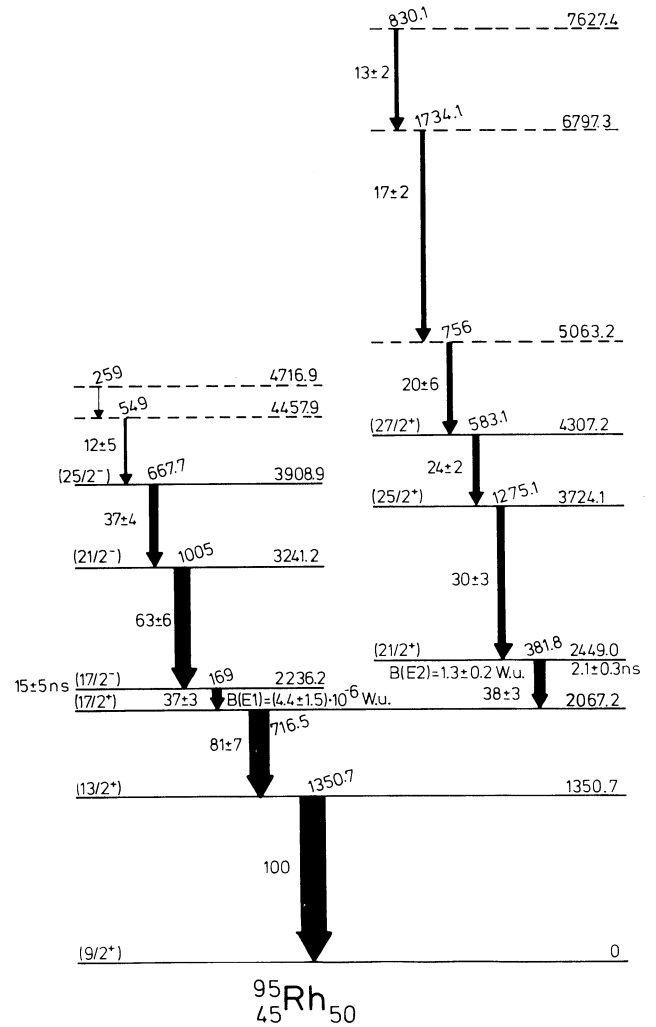


Fig. 2: Level Scheme of  $^{95}\text{Rh}$

#### 3.1.2 The Decay Scheme of $^{95}\text{Pd}^m$

In the  $\gamma$  spectra of the residual activities we observed the transitions below the  $(21/2^+)$  and the  $(17/2^-)$  state with a half-life of  $14 \pm 1$  s <sup>4)</sup>. This activity was assigned to the new isotope  $^{95}\text{Pd}^m$  (see Fig. 3). For the ratio of the production cross sections of the n2p and 3p evaporation channels we obtained

$$\sigma(2np; ^{95}\text{Pd}^m) / \sigma(3p; ^{95}\text{Rh}) = 0.06 \pm 0.02$$

for a beam energy of 135 MeV.  $^{95}\text{Pd}^m$  should have positive parity and a high spin value around 21/2. From level energy systematics (and also from the spectrum of the  $\beta$  decayed protons (see Fig. 4)) we deduced an excitation energy of  $\approx 2$  MeV for  $^{95}\text{Pd}^m$ . The  $Q_{EC}$  (g.s.) value between  $^{95}\text{Pd}^m$  and  $^{95}\text{Rh}$  (g.s.) is then estimated to be  $(8.2 \pm 2) \text{ MeV} = 10.2 \text{ MeV}$  <sup>5)</sup>. With this  $Q_{EC}$  value we obtain a log ft value of  $\approx 5.5$  for the  $\beta$  transition to the  $(21/2^+)$  state in  $^{95}\text{Rh}$ . This log ft value is typical for an allowed  $\beta$  transition. The  $17/2^-$  state in  $^{95}\text{Rh}$  cannot be fed directly by  $\beta$  decay so strongly. For this state we have to assume an indirect feeding.

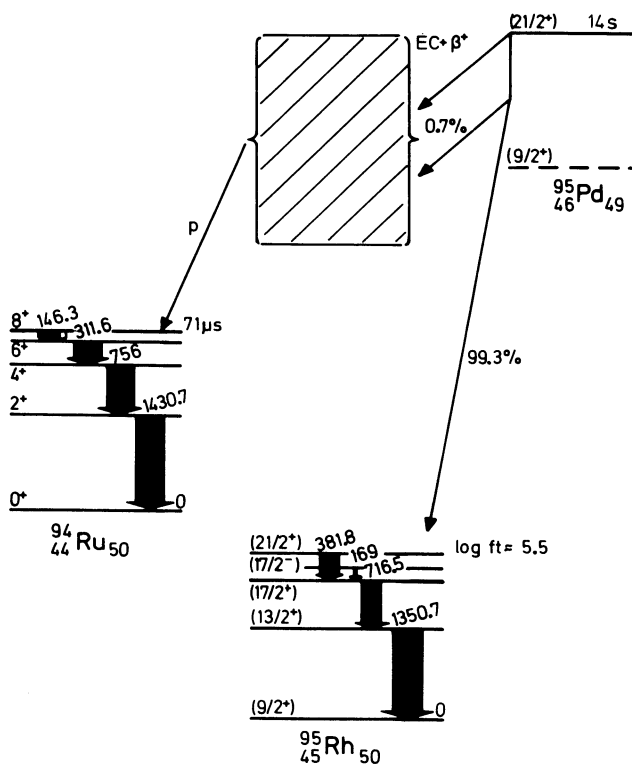


Fig. 3 Decay scheme of  $^{95}\text{Pd}^m$

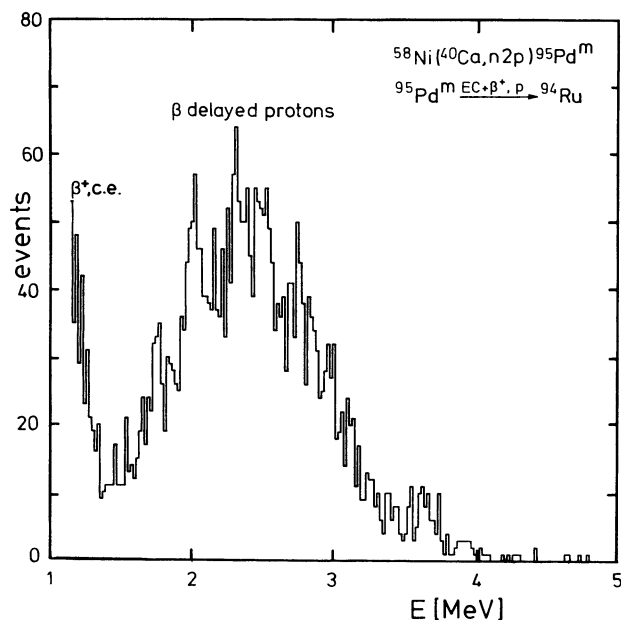


Fig. 4 Energy spectrum of the  $\beta$  delayed protons.

$^{95}\text{Pd}^m$  is expected to be a  $\beta$  delayed proton precursor. If we assume an excitation energy of 2 MeV for  $^{95}\text{Pd}^m$  the predicted maximum proton energy  $Q_{\text{EC}-\beta\text{p}}$  is equal to 4.5 MeV <sup>5)</sup> for a proton decay to the  $8^+$  state at 2644.6 keV in  $^{94}\text{Ru}$  <sup>6)</sup> (see Fig. 3) and would be as high as 7.1 MeV <sup>5)</sup> for a proton decay to the  $^{94}\text{Ru}$  ground state.

Fig. 4 shows the particle spectrum that was taken in a multi spectrum analysis within the first 14s after a 14s irradiation. The spectrum consists of a strong low energy peak below 1.3 MeV caused by positrons and conversion electrons and the proton distribution between 1.3 and 5 MeV. High energy protons with energies over 5 MeV were not observed. The measured half-life of the protons of  $14.2 \pm 2.4$  s fits well the half-life of  $14.1$  s of  $^{95}\text{Pd}^m$ . The contamination of the proton spectrum by other (possible)  $\beta$  delayed proton precursors should be small since the production cross sections for these proton precursors (e.g.  $^{96}\text{Ag}$ ,  $^{94}\text{Rh}$ ,  $^{93}\text{Pd}$ ,  $^{93}\text{Ru}$  and  $^{91}\text{Ru}$ ) are weak compared to the yield of  $^{95}\text{Pd}$  or since the total  $\beta$  branching to proton emitting states is expected to be small.

For  $^{95}\text{Pd}^m$  the total  $\beta$  branching to proton emitting states was determined to be

$$\text{BR}_p = (7.4 \pm 1.9) \cdot 10^{-3}.$$

The measured proton spectrum suggests a feeding of the excited  $71 \mu\text{s}$   $8^+$  state at 2644.6 keV in  $^{94}\text{Ru}$  <sup>6)</sup> (see Fig. 3) through the proton decay. Fig. 5 shows the  $\gamma$  spectrum taken in delayed (5-75  $\mu\text{s}$ ) coincidence with the  $\beta$  delayed protons. The  $\gamma$  transitions below the  $71 \mu\text{s}$   $8^+$  state in  $^{94}\text{Ru}$  were observed. A feeding of the  $10^+$  or the  $12^+$  state in  $^{94}\text{Ru}$  <sup>3)</sup> was not observed.

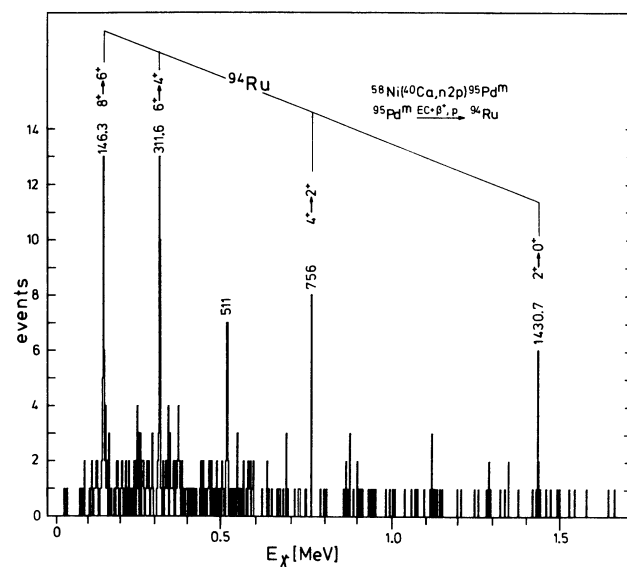


Fig. 5  $\gamma$  spectrum in delayed (5-75  $\mu\text{sec}$ ) coincidence with the  $\beta$  delayed protons.

Fig. 6 shows the TAC time decay curve of the  $\gamma$  radiation relative to the emission time of the  $\beta$  delayed protons. Prompt events are not drawn. The measured half-life of  $79 \pm 23 \mu\text{s}$  fits well the known half-life of  $71 \mu\text{s}$  of the  $8^+$  state in  $^{94}\text{Ru}$ .

The proton spectrum with which the  $\gamma$  radiation in  $^{94}\text{Ru}$  is in delayed coincidence (5-75  $\mu\text{s}$ ) is within the statistics the same as the proton singles spectrum shown in Fig. 4.

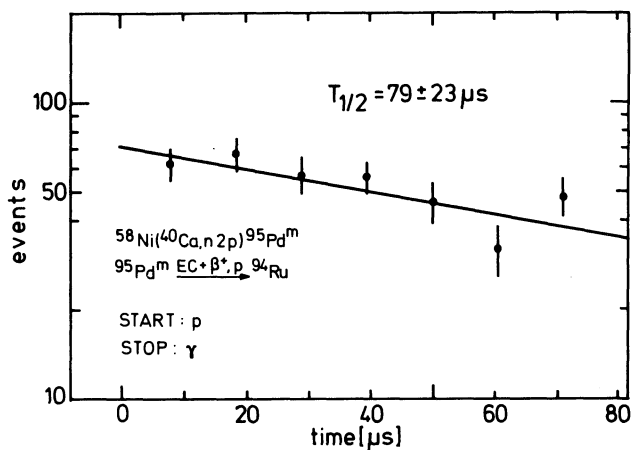


Fig. 6 TAC time decay curve of the  $\gamma$  radiation in  $^{94}\text{Ru}$  relative to the time of emission of the  $\beta$  delayed protons.

To explain the long half-life of  $^{148}\text{Dy}$  of  $^{95}\text{Pd}^m$  we have to assume that  $^{95}\text{Pd}^m$  is not deexcited by electromagnetic dipole or quadrupole radiation. This means that in  $^{95}\text{Pd}$  the  $21/2^+$  state should be below or very close to the  $17/2^+$  state and the  $17/2^-$  state. Ogawa <sup>7)</sup> has shown that in shell model calculations with  $^{100}\text{Sn}_{50}$  as core and with four proton holes and one neutron hole in the  $1g_{9/2}$  subshell it is possible to obtain the  $21/2^+$  state below the  $17/2^+$  state. The E4-E2 cascade deexciting the  $21/2^+$  level via the  $13/2^+$  state to the  $9/2^+$  state could not yet be identified.

### 3.2 N=82 Region

Very proton rich N=82 isotones and neighbouring nuclei were studied with the postaccelerated Ni beams and Zr or Mo targets. At beam energies immediately above the Coulomb barrier the 2p evaporation is the strongest channel. At a beam energy of 250 MeV the 3p channel is strongest. Fig. 7 shows the yields of the identified residual nuclei for the system  $^{58}\text{Ni} + ^{94}\text{Mo}$  at a beam energy of 250 MeV. The compound nucleus in this case is  $^{152}\text{Yb}$ . Also drawn in Fig. 7 are the lightest producible compound nuclei in the considered region. The determination of the mass of  $^{148}\text{Dy}$  with the help of the measurement of the K/ $\beta$  ratio has been already published <sup>8)</sup>.

#### 3.2.1 The Level Scheme of $^{146}\text{Dy}$

$^{146}\text{Dy}$  was studied with the help of the reaction  $^{90}\text{Zr}(^{58}\text{Ni}, 2p)$ . A sequence of levels with the spins  $0^+, 2^+, (4^+), (3^-), (5^-), (7^-)$  and two higher lying levels with the tentatively assigned spins  $(7^-, 8^-, 9^-)$  were identified (see Fig. 8). All transitions in  $^{146}\text{Dy}$  were observed with a half-life of  $150 \pm 40$  ms. (See also the decay scheme  $^{146}\text{Ho} \rightarrow ^{146}\text{Dy}$ ). Energy and spin of this isomeric level are not yet identified.

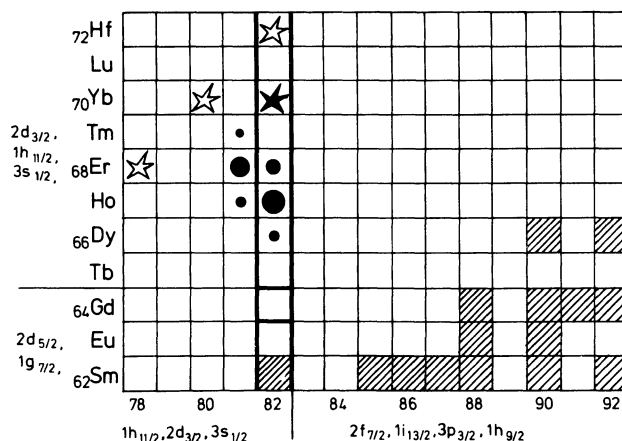


Fig. 7 Relevant part of the nuclear chart with the N=82 region. The compound nucleus of the system  $^{58}\text{Ni} + ^{94}\text{Mo}$  is  $^{152}\text{Yb}$  (full star). Circles indicate the yields of the residual nuclei at a beam energy of 250 MeV. Hollow stars indicate the lightest producible compound nuclei.

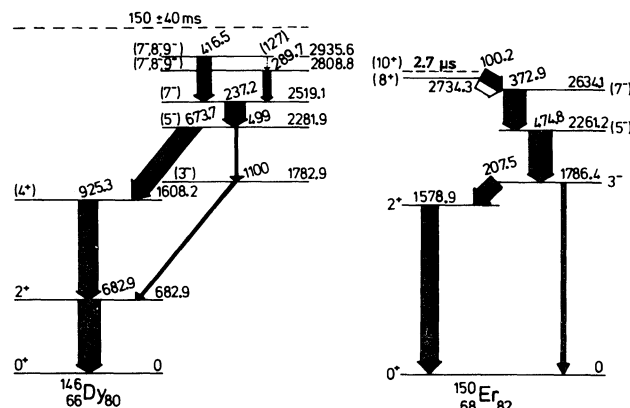


Fig. 8 The level schemes of  $^{146}\text{Dy}$  and  $^{150}\text{Er}$ .

#### 3.2.2 The Level Scheme of $^{150}\text{Er}$

This nucleus was produced in the reactions  $^{94}\text{Mo}(^{58}\text{Ni}, 2p)$  and  $^{92}\text{Mo}(^{60}\text{Ni}, 2p)$ .

Fig. 8 shows the tentative level scheme of  $^{150}\text{Er}$ . Levels with the spins  $0^+, 2^+, 3^-, (5^-), (7^-)$  and  $(8^+)$  were found. If we assume in  $^{150}\text{Er}$  the same  $B(E3, 3^- \rightarrow 0^+)$  value of 37 W.u. as in  $^{146}\text{Gd}$  we deduce a  $B(E1, 3^- \rightarrow 2^+)$  value of  $3 \cdot 10^{-4}$  W.u. from the measured branching  $3^- \rightarrow 0^+$  and  $3^- \rightarrow 2^+$ .

All identified transitions in  $^{150}\text{Er}$  were observed with a half-life of  $2.7 \pm 0.6 \mu\text{s}$  versus the bunched beam. This half-life was tentatively assigned to the  $10^+$  state. The  $10^+ \rightarrow 8^+$  transition is not yet identified. Because of the strong conversion the  $B(E2, 10^+ \rightarrow 8^+)$  value does not depend very much from the transition energy for energies smaller than 100 keV. If we assume a

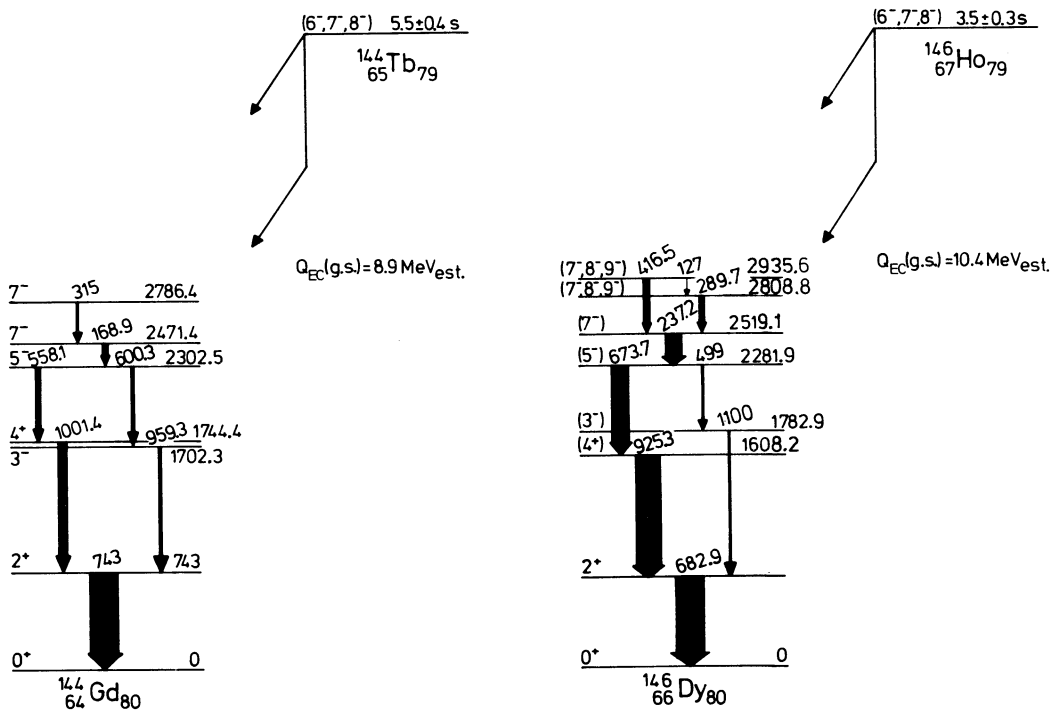


Fig. 9: The  $\beta$  decay schemes of  $^{144}\text{Tb}$  and  $^{146}\text{Ho}$ .

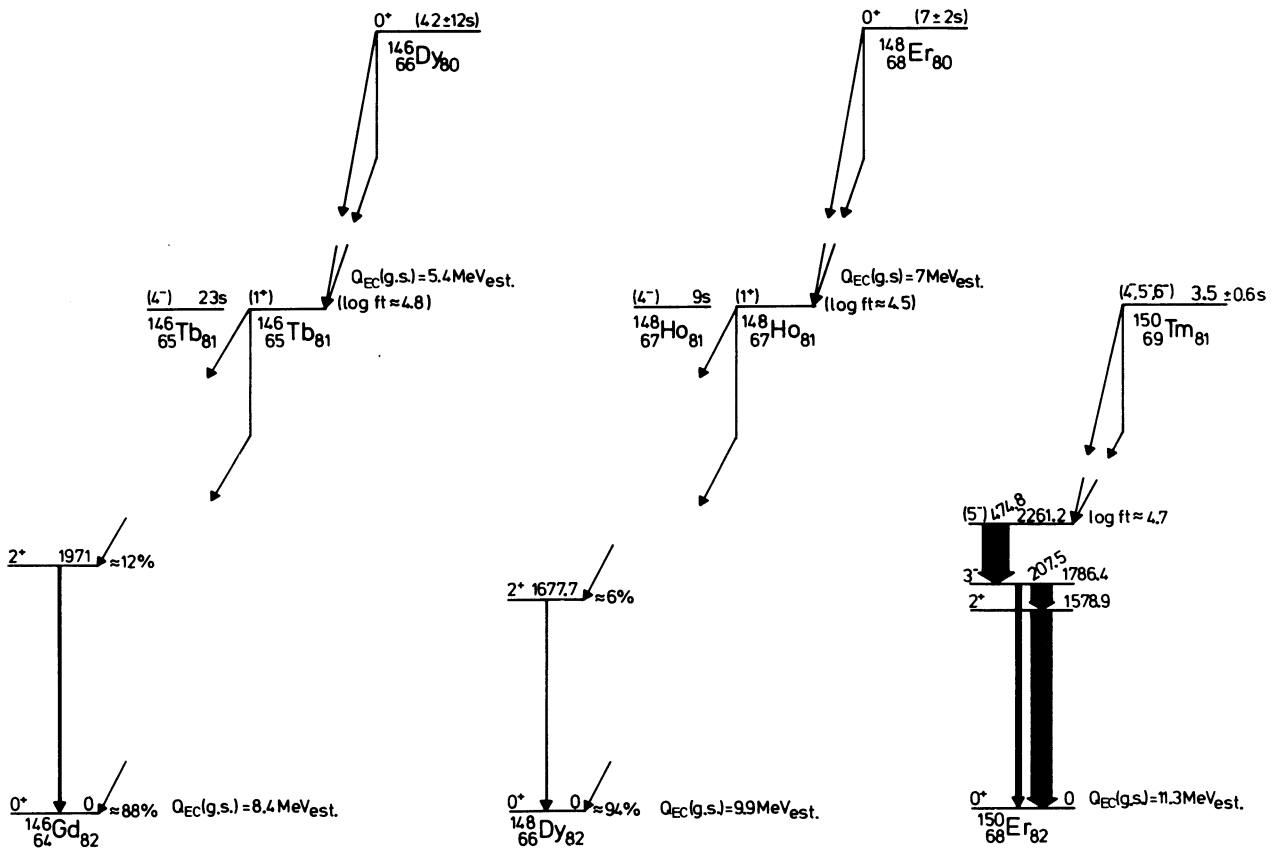


Fig. 10: The  $\beta$  decay schemes and  $^{146}\text{Dy} \rightarrow ^{146}\text{Tb} \rightarrow ^{146}\text{Gd}$ ,  $^{148}\text{Er} \rightarrow ^{148}\text{Ho} \rightarrow ^{148}\text{Dy}$  and  $^{150}\text{Tm} \rightarrow ^{150}\text{Er}$ .

$10^+ \rightarrow 8^+$  transition of 60 keV a  $B(E2, 10^+ \rightarrow 8^+)$  value of 0.25 W.u. is obtained. In  $^{148}\text{Dy}$  the  $B(E2, 10^+ \rightarrow 8^+)$  value is 0.9 W.u. According to shell model calculations <sup>9)</sup> for  $(h_{11/2})_v^2$  configurations these  $B(E2)$  values are predicted to be  $\propto (6-n)^2/(6-2)^2$ . The measured values agree well with the prediction.

### 3.2.3 The $\beta$ Decay Schemes of $^{144}\text{Tb}$ and $^{146}\text{Ho}$

In the residual activities of the system  $^{58}\text{Ni} \rightarrow ^{90}\text{Zr}$  we observed the  $\gamma$  transitions below the second  $7^-$  state in  $^{144}\text{Gd}$  ( $10^-$ ) with a half-life of  $5.5 \pm 0.4$  s and the  $\beta$  transitions below the 2935.6 keV level in  $^{146}\text{Dy}$  with a half-life of  $3.5 \pm 0.3$  s. These activities were assigned to the new isotopes  $^{144}\text{Tb}$  and  $^{146}\text{Ho}$  (Fig. 9). The observed transitions in  $^{146}\text{Dy}$  are in prompt coincidence with the annihilation radiation. With the help of log ft values we obtain negative parity and a spin value around  $7\hbar$  for  $^{144}\text{Tb}$  and  $^{146}\text{Ho}$ .

### 3.2.4 The $\beta$ Decay Schemes $^{146}\text{Dy} \rightarrow ^{146}\text{Tb} \rightarrow ^{146}\text{Gd}$ , $^{148}\text{Er} \rightarrow ^{148}\text{Ho} \rightarrow ^{148}\text{Dy}$ and $^{150}\text{Tm} \rightarrow ^{150}\text{Er}$

The spins of  $^{146}\text{Tb}$  (23s) and  $^{148}\text{Ho}$  (9s) are known to be  $4^-$  (6, 11). In the residual activities of the systems  $^{58}\text{Ni} \rightarrow ^{90}\text{Zr}$  and  $^{58}\text{Ni} \rightarrow ^{92}\text{Mo}$  we observed a  $\beta$  decaying ( $1^+$ ) state in  $^{146}\text{Tb}$  and  $^{148}\text{Ho}$ , respectively (see Fig. 10). These  $1^+$  states are produced in the  $\beta$  decays of  $^{146}\text{Dy}$  and  $^{148}\text{Er}$ . The ( $1^+$ ) states in  $^{146}\text{Tb}$  and  $^{148}\text{Ho}$  decay mainly to the ground states and by about 10% to the excited  $2^+$  states in  $^{146}\text{Gd}$  and  $^{148}\text{Dy}$ , respectively. From  $Q_{EC}$  value considerations the measured half-lives for the  $2^+$  states were tentatively assigned to the activities  $^{146}\text{Dy}$  and  $^{148}\text{Er}$ .

In the residual activities of the system  $^{60}\text{Ni} \rightarrow ^{92}\text{Mo}$  the  $\gamma$  transitions below the ( $5^-$ ) state in  $^{150}\text{Er}$  were observed with a half-life of  $3.5 \pm 0.6$  s (see Fig. 10). This activity was assigned to  $^{150}\text{Tm}$  which is produced in the reaction  $^{92}\text{Mo}(^{60}\text{Ni}, pn)$ . From the log ft values we obtain a spin of ( $4^-, 5^-, 6^-$ ) for  $^{150}\text{Tm}$  (3.5s).

### 3.2.5 The $\beta$ decay scheme $^{150}\text{Er} \rightarrow ^{150}\text{Ho} \rightarrow ^{150}\text{Dy}$

$^{150}\text{Er}$  was found to decay with a half-life of 18.5s to the excited ( $1^+$ ) state in  $^{150}\text{Ho}$  (log ft = 3.6) which is deexcited via the 475.8 keV  $\gamma$  transition to the ( $2^-$ ) state (Fig. 11). This  $\beta$  decay is analogous to the  $\beta$  decay of  $^{148}\text{Dy}$ . The  $Q_{EC}(\text{g.s.})$  value for the  $\beta$  decay of  $^{150}\text{Er}$  was measured to be  $4030 \pm 80$  keV with the help of the determination of the  $K/\beta$  ratio (the method is described in Ref. 8). The  $2^-$  state in  $^{150}\text{Ho}$  decays with a half-life of  $72 \pm 10$  s to  $^{150}\text{Dy}$ . In this  $\beta$  decay the  $4^+$  and the ( $3^-$ ) state in  $^{150}\text{Dy}$  are populated. Our decay scheme of  $^{150}\text{Ho}$  is in agreement with Ref. 12.

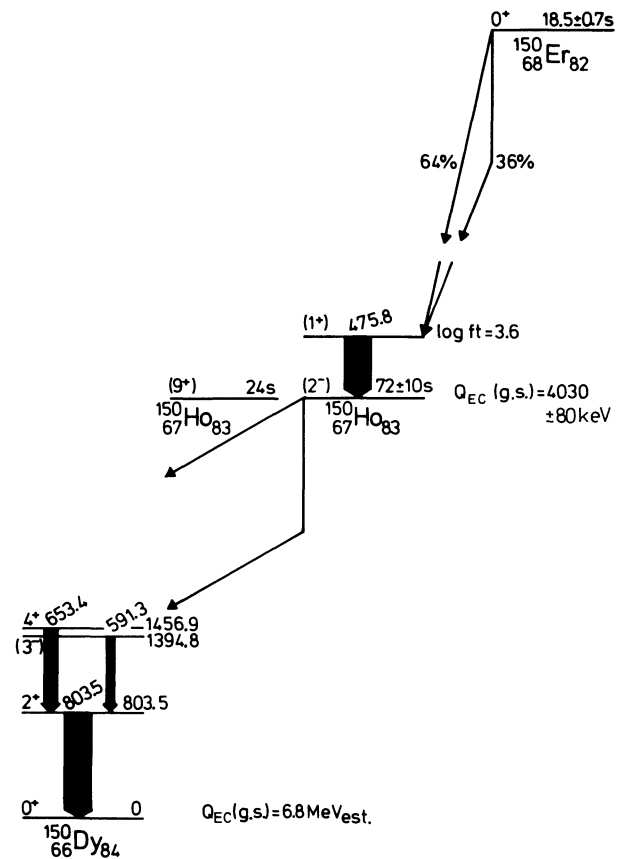


Fig. 11 The  $\beta$  decay scheme  $^{150}\text{Er} \rightarrow ^{150}\text{Ho} \rightarrow ^{150}\text{Dy}$ .

### Acknowledgement

The authors would like to thank Dr. K. Ogawa for sending his calculations before publication.

### References

- 1) E. Nolte, G. Geschonke, K. Berdermann, R. Oberschmid, R. Zierl, M. Feil, A. Jahnke, M. Kress and H. Morinaga, Nucl. Instr. Meth. 158, 311 (1979)
- 2) E. Nolte, G. Geschonke, K. Berdermann, M. Kress, W. Schollmeier, Y. Shida, H. Morinaga, IEEE Trans. Nucl. Sci. 26, 3724 (1979)
- 3) E. Nolte, G. Korschinek, U. Heim, Z. Physik A 298, 191 (1980)
- 4) E. Nolte and H. Hick, Phys. Lett. 97B, 55 (1980)
- 5) P.A. Seeger and W.M. Howard, At. Data Nucl. Data Tables 17 (1976)
- 6) C.M. Lederer and V.S. Shirley, eds. Table of isotopes (Wiley, New York, 1978)
- 7) K. Ogawa (Institute for Nuclear Study, Tokyo) priv. comm.
- 8) L. Spanier, S.Z. Gui, H. Hick and E. Nolte, Z. Physik A 299, 113 (1981)
- 9) R.P. Lawson, to be published in Z. Physik

- 10) M.A.J. Mariscotti, H. Beuscher, W.F. Davidson, Y. Gono, H.M. Jäger, R.M. Lieder, M. Müller-Veggian, A. Neskakis, D.R. Zolnowski, Ann. Report KFA Jülich-IKP, p. 37 (1976)
- 11) K.S. Toth, C.R. Bingham, D.R. Zolnowski S.E. Cala, H.K. Cater, D.C. Sousa, Phys. Rev. C18, 482 (1979)
- 12) C.F. Liang, P. Paris, A. Peghaire and H. Szichman, Z. Physik A297, 303 (1980)

#### DISCUSSION

*P.J. Daly:* 1) We too have been marching up the N=82 shell, investigating the interactions of the  $h_{11/2}$  valence protons outside Z=64, with heavy ion beams from the Argonne Linac. For  $^{150}\text{Er}$  we find the branching intensity  $3^- \rightarrow 0^+$  to be not more than 4%; could the much larger intensity that you report arise from coincidence summing? 2) We have found that elusive  $10^+ \rightarrow 8^+$  ( $\pi h_{11/2}$ )<sup>4</sup> transition in  $^{150}\text{Er}$  ( $\pi h_{11/2}$ )<sup>4</sup> its energy is 63 keV. With the  $10^+$  half-life of 2.5  $\mu\text{s}$ , this gives a B(E2) of 11.6 e<sup>2</sup>fm<sup>4</sup>, just about exactly the predicted factor of 4 smaller than the value we obtained earlier (Z.Physik A288 (1978) 103; *ibid.* A298 (1980) 173) for the  $10^+ \rightarrow 8^+$  ( $\pi h_{11/2}$ )<sup>2</sup> transition in  $^{148}\text{Dy}$ .

*E. Nolte:* The shown intensities in the level scheme of  $^{150}\text{Er}$  are preliminary results.